Prediction of binding free energy for adsorption of antimicrobial peptide lactoferricin B on a POPC membrane

Victor Vivcharuk[*]

Biophysics Interdepartmental Group and Department of Physics, University of Guelph, Guelph, Ontario N1G 2W1, Canada

Bruno Tomberli[†]

Department of Physics and Astronomy, Brandon University, Brandon, Manitoba R7A 6A9, Canada

Igor S. Tolokh[‡]

Department of Physics, University of Guelph, Guelph, Ontario N1G 2W1, Canada

C. G. Gray[§]

Guelph-Waterloo Physics Institute and Department of Physics, University of Guelph, Guelph, Ontario N1G 2W1, Canada

Molecular dynamics (MD) simulations are used to study the interaction of a zwitterionic palmitoyl-oleoyl-phosphatidylcholine (POPC) bilayer with the cationic antimicrobial peptide bovine lactoferricin (LFCinB) in a 100 mM NaCl solution at 310 K. The interaction of LFCinB with POPC is used as a model system for studying the details of membrane-peptide interactions, with the peptide selected because of its antimicrobial nature. Seventy-two 3 ns MD simulations, with six orientations of LFCinB at 12 different distances from a POPC membrane, are carried out to determine the potential of mean force (PMF) or free energy profile for the peptide as a function of the distance between LFCinB and the membrane surface. To calculate the PMF for this relatively large system a new variant of constrained MD and thermodynamic integration is developed. A simplified method for relating the PMF to the LFCinB-membrane binding free energy is described and used to predict a free energy of adsorption (or binding) of -1.05 ± 0.39 kcal/mol, and corresponding maximum binding force of about 20 pN, for LFCinB-POPC. The contributions of the ions-LFCinB and the water-LFCinB interactions to the PMF are discussed. The method developed will be a useful starting point for future work simulating peptides interacting with charged membranes and interactions involved in the penetration of membranes, features necessary to understand in order to rationally design peptides as potential alternatives to traditional antibiotics.

I. INTRODUCTION

The interactions of peptides with biological membranes have been studied for a number of years, for the purpose of understanding the mechanism of action for membrane-active peptides as well as for designing peptides which can modulate membrane properties. (A compendium of many such peptides studied to date is available [1].) One of the goals is to find possible alternatives to traditional antibiotics. Certain antimicrobial peptides can specifically target their activity against the membranes of microbes with minimal harm to the membranes of plants and animals (for reviews see, e.g., [2,3]). A basic model that explains the selectivity of most antimicrobial peptides on cell surfaces is based on the differences in macromolecular constitution, structure, and charge distribution of bacterial and eukaryotic membranes. For example, gram-negative bacterial cell envelopes consist of a cytoplasmic membrane, a peptidoglycan layer, and an outer membrane whose outer leaflet is constituted mainly of lipopolysacharides with negatively charged headgroups. In contrast, the outer leaflet of most mammalian membranes is composed of lipids with no net charge. The small number of the negatively charged lipids are segregated into the inner leaflet [4]. Because almost all active peptides contain hydrophyllic and basic amino acids, they can selectively interact with anionic bacterial membranes via coulombic interaction. The similarities between many cationic antimicrobial peptides (CAPs), which are short, highly cationic, and stabilized by disulphide bonds, possibly belie the many mechanisms by which they may act. In this study, bovine Lactoferricin (LFCinB), a 25-residue antimicrobial peptide with a single disulfide crosslink highly enriched with aromatic and basic amino acids (two tryptophans, two phenylalanines and eight basic residues), is used to represent a typical CAP.

CAP interactions with real membranes are poorly understood. Therefore studies with model membranes clearly provide important information for CAPs that target bacterial membranes. However, even CAPs that disrupt intracellular targets must pass through the bacterial membrane. The mechanics of this process is still unknown at the molecular level.

In this paper we investigate the interaction of LFCinB with the neutral palmitoyl-oleoyl-phosphatidylcholine (POPC) membrane. We rederive more simply the binding

─────────

[*]viv@physics.uoguelph.ca
[†]tomberlib@brandonu.ca
[‡]tolokh@physics.uoguelph.ca
[§]cgg@physics.uoguelph.ca

thermodynamics formalism, establish a new simulation algorithm for the potential of mean force (PMF), test the algorithm on solvated Na$^+$, Cl$^-$ and apply it to the solvated LFCinB-POPC system. Later work will investigate CAP interactions with a charged (anionic) palmitoyl-oleoyl-phosphatidylglycerol (POPG) membrane, because phosphatidyl-glycerols are one of the major constituents of bacterial membranes while erythrocyte membranes and most other eukaryotic membranes are generally made up of phosphatidyl-cholines (PCs) [5]. In this first study we also restrict ourselves to surface (or adsorption) interactions. Subsequent work will deal with membrane penetration.

The solution structure of LFCinB is known from NMR spectroscopy [6]. LFCinB is a 25-amino acid peptide released by pepsin cleavage of the bovine milk protein lactoferrin with the amino acid sequence FKCRR WQWRM KKLGA PSITC VRRAF in the single letter code, and contains a single disulfide crosslink between residues 3 and 20. In solution, LFCinB loses the alpha-helical structure found in lactoferrin and it adopts a twisted beta-sheet structure with high amphiphilicity. It has been shown [5] that the Trp6 and Trp8 residues and several cationic Arg residues are important for the antimicrobial activity. It also has been discovered [7] that the Arg residues near the N-terminus of the human lactoferrin are very important for membrane interactions. With all-atom models for the membrane, peptide, and water, the molecular dynamics (MD) simulations reported in this work provide essential data for understanding the membrane-peptide interaction.

Membrane-peptide binding thermodynamics formalism is sketched in Secs. II A and II B. The statistical mechanics of binding was greatly enlightened by Gilson *et al.* [8] who clarified the role of standard states and for strong binding also showed the nondependence of the binding free energy on the somewhat arbitrary definition of "bound" and "free" species. For the case of adsorption, Ben-Tal *et al.* [9] simplified the discussion by noting that, in classical treatments, the kinetic parts of the partition functions can be eliminated at the beginning, and one can derive the thermodynamic adsorption observables from just the configurational partition functions. We further simplify the discussion by showing that the configurational partition functions can also be taken into account more simply and implicitly. We express the adsorption observables in terms of the single-molecule reduced distribution functions $P(z)$ and $P(z,\Omega)$. Here $P(z)$ is the probability density to find the peptide center of mass at distance z from the membrane, irrespective of peptide orientation, and $P(z,\Omega)$ is the probability density to find the peptide at distance z and orientation Ω. The distribution functions themselves, $P(z)$ and $P(z,\Omega)$, can be calculated directly from the corresponding PMF's, $W(z)$ and $W(z,\Omega)$, respectively. A new algorithm is developed to calculate the PMFs, a variant of constrained MD and thermodynamic integration, and is described in Sec. II C. From the PMF's we predict the binding free energy for LFCinB adsorbed on a POPC membrane. Results and discussion follow in later sections.

II. THEORY

A. Distribution functions and the potential of mean force

Consider the schematic binding geometry of Fig. 1, which approximates that of a giant vesicle. We have an equilibrium
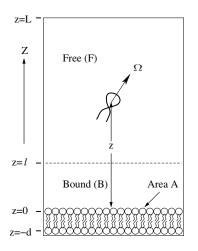

FIG. 1. Schematic binding geometry. The peptide has center of mass z coordinate z and orientation Ω. There are $N=N_F+N_B$ peptides in a box of volume $V \simeq LA=V_F+V_B$, where $z=l$ divides the free (F) and bound (B) volumes. The box length in the z direction is approximately L and the area of the x, y plane in the transverse direction is A. The solvent (water, not shown) also contains Na$^+$ and Cl$^-$ ions (not shown). The origin $z=0$ is chosen at the membrane surface (average position of head group phosphorous atoms) since here we consider only adsorption (not absorption). The distance d (=36.8 Å for POPC) is the mean distance between the head-group phosphorous atoms in the two membrane leaflets.

system of N identical peptide molecules dissolved in a solvent (water) of a volume $V \simeq AL$ (see Fig. 1) and temperature T containing ions (Na$^+$, Cl$^-$) and a binding surface (the membrane). The solution is assumed dilute so that we can neglect peptide-peptide interactions. Peptides are considered to be bound (B) if $z<l$ and free (F) if $z>l$, where z is the z coordinate of the center of mass of the peptide, and where the choice of l is discussed below. The densities of bound and free peptides are $\rho_B=N_B/V_B$ and $\rho_F=N_F/V_F$, respectively, where $V_B=A(l-l')$ and $V_F=A(L-l) \approx AL=V$, since $l \ll L$ and l' defines an effective excluded volume (Al') for the peptide center of mass position related to the choice of $z=0$. In the case of surface adsorption, when there is a substantial barrier for peptide molecules to penetrate into the lipid head group region, and with $z=0$ defined by us as the average position of phosphorus atoms, the excluded volume is connected with the size of the peptide and lipid head groups. Our main objective is to calculate the equilibrium binding constant $K=\rho_B/\rho_F$ and related adsorption free energy ΔG^0.

Because the solution is assumed to be dilute, at this stage we need only consider one peptide. We denote the system Cartesian coordinates by $(\mathbf{r}_1,\mathbf{r}_2,\dots,\mathbf{r}_n)$, where $\mathbf{r}_i=(x_i,y_i,z_i)$ denotes the Cartesian coordinates of atom i of the system, and $i=1,\dots,n$ runs over all n atoms constituting the system, i.e., a single peptide molecule, the solvent molecules, the ions, and the lipid molecules constituting the membrane. We assume that classical statistical mechanics applies to all degrees of freedom, so that the normalized configurational probability distribution function is given by

$$P(\mathbf{r}_1, \ldots, \mathbf{r}_n) = e^{-\beta U(\mathbf{r}_1, \ldots, \mathbf{r}_n)}/Z, \tag{1}$$

where $\beta = 1/k_B T$ with k_B Boltzmann's constant, $U(\mathbf{r}_1, \ldots, \mathbf{r}_n)$ is the system total potential energy (intra- and intermolecular), and

$$Z = \int e^{-\beta U(\mathbf{r}_1, \ldots, \mathbf{r}_n)} d\mathbf{r}_1 \cdots d\mathbf{r}_n \tag{2}$$

is the configurational partition function. Instead of considering all Cartesian coordinates for the peptide atoms, we introduce the peptide center of mass coordinates $\mathbf{r} = (x, y, z)$ and peptide orientation coordinates Ω (e.g., Euler angles ϕ, θ, χ) to replace six of the peptide Cartesian coordinates. The set of system coordinates is now denoted by $(\mathbf{r}, \Omega, q)$, where q denotes all other system coordinates, i.e., peptide internal (vibrational) coordinates, solvent coordinates, ion coordinates, and membrane atom coordinates. The corresponding probability distribution function $P(\mathbf{r}, \Omega, q)$ can be derived from $P(\mathbf{r}_1, \ldots, \mathbf{r}_n)$ by the change of variables $(\mathbf{r}_1, \ldots, \mathbf{r}_n) \to (\mathbf{r}, \Omega, q)$. The transformation involves a Jacobian determinant (see the Appendix).

As we shall see, for the purpose of calculating the binding thermodynamic observables, we can restrict our attention to the single-molecule reduced distribution functions $P(z, \Omega)$ and $P(z)$, obtained from $P(\mathbf{r}, \Omega, q)$ by integration over all variables not specified in the arguments of $P(z, \Omega)$ and $P(z)$, i.e.,

$$P(z, \Omega) = \int dx\,dy\,dq\,P(\mathbf{r}, \Omega, q), \tag{3}$$

$$P(z) = \int dx\,dy\,d\Omega\,dq\,P(\mathbf{r}, \Omega, q). \tag{4}$$

Physically, $P(z, \Omega)$ is the probability density to find the peptide at distance z from the membrane and with orientation Ω, and $P(z)$ is the probability density to find the peptide at distance z irrespective of orientation. From the definition of a PMF (see the Appendix) these reduced distribution functions can be expressed in terms of the PMF's $W(z, \Omega)$ and $W(z)$ by

$$P(z, \Omega) = e^{-\beta W(z, \Omega)}/(8\pi^2 L), \tag{5}$$

$$P(z) = e^{-\beta W(z)}/L, \tag{6}$$

where we have assumed that the range of $W(z, \Omega)$, which is nonzero due to the presence of the membrane, is small compared to L, so that the normalizing denominators in Eqs. (5) and (6) simplify, since $\int dz\,e^{-\beta W(z, \Omega)} \approx L$ and we have also used $\int d\Omega = 8\pi^2$. Note that far into the bulk solution we have $P(z, \Omega) \approx 1/(8\pi^2 L)$ and $P(z) \approx 1/L$, the constants expected intuitively. The orientation-dependent PMF $W(z, \Omega)$ and orientation-independent PMF $W(z)$ are seen from Eqs. (5) and (6) and $P(z) = \int d\Omega\,P(z, \Omega)$ to be related by

$$e^{-\beta W(z)} = \int \frac{d\Omega}{8\pi^2} e^{-\beta W(z, \Omega)}. \tag{7}$$

We note that $\exp[-\beta W(z)]$ is an unweighted orientational average of $\exp[-\beta W(z, \Omega)]$; only at high temperatures does

$W(z)$ reduce to a simple orientational average of $W(z, \Omega)$.

Returning to the dilute solution with N independent peptides, we denote the local peptide density (average number of peptides per unit volume) by $\rho(z)$ and then use $\rho(z)A\,dz = NP(z)\,dz$ and Eq. (6) to find

$$\rho(z) = \rho e^{-\beta W(z)} \approx \rho_F e^{-\beta W(z)}, \tag{8}$$

where $\rho = N/V \simeq N_F/V_F = \rho_F$. The excess over the average number of peptides in the horizontal slab at z of volume $A\,dz$ is $[\rho(z) - \rho_F]A\,dz$. The Gibbs surface excess density Γ (per unit area) is thus

$$\Gamma = \rho_F \int_{l'}^{\infty} (e^{-\beta W(z)} - 1)\,dz, \tag{9}$$

since for large L the true upper limit L in Eq. (9) can be replaced by ∞ due to the fact that $\exp[-\beta W(z)] \to 1$ for $W(z) \to 0$ as it does for $z \gtrsim$ range of $W(z)$. For adsorption the lower limit l' is defined by the relation $W(z) \le 0$ for $z \ge l'$ and is connected with the excluded volume due to the sizes of the peptide and lipid head groups. We assume we are dealing with stable adsorption, where $W(z) > 0$ for $z \le l'$. l' depends of the choice of the origin of the coordinate system but $\Delta l = l - l'$ does not.

We now discuss the choice of l, the dividing line between what we define as free and bound peptide (see Fig. 1). As discussed by Gilson *et al.* [8], for strong binding ($\beta|W| \gg 1$) the thermodynamic observables are insensitive to the precise value chosen if l is chosen close to the range of $W(z)$. Gilson *et al.* [8] show this using the binding free energy $\Delta G^0 = -k_B T \ln(\rho_B/\rho_F)$ (see the next section). The same point can be seen from Eq. (9), where replacement of ∞ by any choice of $l >$ range of $W(z)$ gives the correct result for Γ for strong binding. We see that for thermodynamic properties the choice $l \approx$ range of $W(z)$ is appropriate. For other properties, other choices may be more suitable. Thus for a fluorescence quenching experiment, the choice $l \approx$ quenching range is the appropriate one. We discuss such applications in future work.

B. Binding thermodynamics and statistical mechanics

As known from both thermodynamics and statistical mechanics [10], for dilute solutions the chemical potential μ_α of solute α depends logarithmically on the number density ρ_α, i.e., $\mu_\alpha = k_B T \ln(C_\alpha \rho_\alpha)$, where C_α is a solute-solvent property with dimensions of inverse density which depends on temperature (T) and pressure (p) but is independent of ρ_α. We apply this relation to two states of the free (F) peptide at the same T and p,

$$\mu_F - \mu_F^0 = k_B T \ln(\rho_F/\rho_F^0), \tag{10}$$

where μ_F and μ_F^0 are the free peptide chemical potentials at the density of interest ρ_F, and some arbitrary reference density ρ_F^0, respectively, both at the given T and p. Note that C_F cancels out. Similarly for the bound (B) peptide we have

$$\mu_B - \mu_B^0 = k_B T \ln(\rho_B/\rho_B^0). \tag{11}$$

The F and B phases are assumed to be in equilibrium at the given T and p, with equilibrium densities ρ_F and ρ_B, and at

equilibrium we have $\mu_B = \mu_F$. This gives from Eqs. (10) and (11)

$$\mu_B^0 - \mu_F^0 = k_B T \ln(\rho_B^0/\rho_F^0) - k_B T \ln(\rho_B/\rho_F). \quad (12)$$

Equation (12) holds for any reference densities ρ_B^0 and ρ_F^0. If we choose $\rho_B^0 = \rho_F^0$, Eq. (12) simplifies to

$$\mu_B^0 - \mu_F^0 = -k_B T \ln(\rho_B/\rho_F) \equiv -k_B T \ln K, \quad (13)$$

where $K = \rho_B/\rho_F$ is the equilibrium binding constant. We define the adsorption (or binding) free energy per molecule by

$$\Delta G^0 \equiv \mu_B^0 - \mu_F^0 = -k_B T \ln K, \quad (14)$$

which has the standard form. Physically, ΔG^0 is seen to be the change in free energy per molecule (chemical potential) in going from a free state at any (dilute) density ρ_F^0 to the bound state at the same density $\rho_B^0 = \rho_F^0$.

A statistical mechanical expression for $K = \rho_B/\rho_F$ is given in terms of the local density $\rho(z)$ using $\rho_B = N_B/V_B = [1/A(l-l')]\int_{l'}^l \rho(z) A dz$ and then Eq. (8) gives in terms of the PMF $W(z)$

$$K = \frac{1}{l-l'} \int_{l'}^l dz e^{-\beta W(z)} \equiv \langle e^{-\beta W} \rangle_{\Delta l}. \quad (15)$$

The lower integration limit l' in Eq. (15) can be replaced by zero since the Boltzmann factor strongly vanishes for $z \lesssim l'$. Thus K is the (unweighted) average of the Boltzmann factor over the range of the binding region $\approx$ range of $W(z)$ (see previous section and below).

Two limiting cases of Eqs. (14) and (15) are illuminating. For weak binding $(\beta|W| \ll 1)$, we can approximate $\exp(-\beta W)$ as $1 - \beta W$ and using $\ln(1+x) \approx x$ for small x we see from Eqs. (14) and (15) that

$$\Delta G^0 \approx \langle W \rangle_{\Delta l} \quad \text{(weak binding)}. \quad (16)$$

In this limit ΔG^0 is a simple average of $W(z)$ over the binding region. The strong binding limit is more relevant to the peptide-membrane systems we study. Assume for simplicity that $W(z)$ has a square well shape

$$W(z) = \begin{cases} \infty & \text{if } z < \sigma_1 \\ -\epsilon & \text{if } \sigma_1 \leq z \leq \sigma_2 \\ 0 & \text{if } z > \sigma_2. \end{cases} \quad (17)$$

Choosing l not too much larger than σ_2, we find from Eqs. (14) and (15)

$$\Delta G^0 \approx -\epsilon - k_B T \ln\left(\frac{\sigma_2 - \sigma_1}{l - l'}\right) - k_B T\left(\frac{l - \sigma_2}{\sigma_2 - \sigma_1}\right) e^{-\beta \epsilon}. \quad (18)$$

For strong binding $(\epsilon \gg k_B T)$ and wells not too narrow we see that Eq. (18) becomes

$$\Delta G^0 \approx -\epsilon \quad \text{(strong binding)}. \quad (19)$$

Note that Eq. (19) is independent of the choices of $z=0$ (defining l') and $z=l$ (defining bound species B), as well as σ_1 and σ_2. We see again that the precise choice of l does not matter [8], as discussed in the previous section. For the

peptide-membrane system studied in this paper we have $\beta W \sim -2$ for z in the region of the well minimum (future work with charged membranes will have $\beta W \sim -10$) and we use the exact expressions Eqs. (14) and (15) since the true shape of $W(z)$ is not square.

The free energy profile $W(z)$ can be decomposed into enthalpic $\Delta H(z)$ and entropic $\Delta S(z)$ components using

$$W(z) = \Delta H(z) - T\Delta S(z), \quad (20)$$

where $\Delta H(z) = \partial[\beta W(z)]/\partial\beta$. From Eq. (7) we find

$$\Delta H(z) \simeq \frac{\int d\Omega e^{-\beta W(z,\Omega)} W(z,\Omega)}{\int d\Omega e^{-\beta W(z,\Omega)}}, \quad (21)$$

where we assume that a temperature-dependent term involving $\partial W(z,\Omega)/\partial\beta$ is small and can be neglected.

A similar decomposition of the binding free energy ΔG^0 can be carried out. The binding enthalpy (heat of reaction) $\Delta H^0 = \partial(\beta \Delta G^0)/\partial\beta$ can be calculated using Eqs. (14) and (15) (replacing l' by zero as explained earlier). We get

$$\Delta H^0 = \frac{\int_0^l dz e^{-\beta W(z)} \Delta H(z)}{\int_0^l dz e^{-\beta W(z)}}, \quad (22)$$

with $\Delta H(z)$ given approximately by Eq. (21), which is equivalent to the corresponding expression in [9]. The adsorption entropy ΔS^0 is obtained from ΔG^0 and ΔH^0 using the relation

$$\Delta G^0 = \Delta H^0 - T\Delta S^0. \quad (23)$$

In deriving Eq. (22) no further assumption is made that the temperature dependence of $W(z)$ is weak; both ΔH^0 and $T\Delta S^0$ include the terms involving $\partial W(z)/\partial\beta$. It should be noted [11] that, unlike ΔG^0 and ΔS^0, ΔH^0 is in fact independent of the choice $\rho_F^0 = \rho_B^0$, as can be seen by obtaining ΔG^0 from the more general expression (12) for $\mu_B^0 - \mu_F^0$.

Because both $\Delta H(z)$ and $W(z)$ are negligible for $z \gtrsim$ range of $W(z)$, the numerator in Eq. (22) is to a good approximation given by $\int_0^\infty dz e^{-\beta W(z)} \Delta H(z)$, and the denominator is to a good approximation $l + \int_0^\infty dz(e^{-\beta W(z)} - 1)$. For strong binding l [range of $W(z)$] is negligible compared to the length $\int_0^\infty dz(e^{-\beta W(z)} - 1)$ and Eq. (22) can be approximated by

$$\Delta H^0 \simeq \frac{\int_0^\infty dz e^{-\beta W(z)} \Delta H(z)}{\int_0^\infty dz(e^{-\beta W(z)} - 1)}, \quad (24)$$

which is manifestly independent of l. An expression of the form (24) has been derived for adsorption on solid surfaces from a dilute gas of atoms, with the potential of mean force $W(z)$ and local enthalpy change $\Delta H(z)$ both replaced by the bare atom-surface potential $U(z)$ [12].

C. Algorithm for the potential of mean force

There are numerous algorithms [13] to compute, in principle, a PMF such as $W(z,\Omega)$, falling into two general classes: (i) obtain $W(z,\Omega)$ from the distribution function $P(z,\Omega)$ using Eq. (5) and (ii) obtain $W(z,\Omega)$ from the mean force $\langle -\partial U/\partial z \rangle_{z,\Omega}$ on the z coordinate using Eq. (A1). Because our system is rather large we use a force method [13] and develop a new variant of constrained MD and thermodynamic integration [14–18].

The PMF $W(z,\Omega)$ is the reversible work required to bring the center of mass of the peptide from any position (say z_0) in the bulk fluid to the position z near the membrane surface, keeping the peptide orientation Ω fixed at all times. Using the relation [see Eq. (A1)] $\bar{F}(z,\Omega) = -\partial W(z,\Omega)/\partial z$, where $\bar{F}(z,\Omega)$ is the mean force (which is in the z direction by symmetry) on the peptide for fixed z and Ω, we can obtain $W(z,\Omega)$ from $\bar{F}(z,\Omega)$ by integration, i.e.,

$$W(z,\Omega) = W(z_0,\Omega) - \int_{z_0}^{z} \bar{F}(z',\Omega) dz'. \qquad (25)$$

If z_0 is deep in the bulk solution, we have $\bar{F}(z_0,\Omega)=0$. We choose our reference free energy for $W(z,\Omega)$ such that $W(z_0,\Omega)=0$ and write Eq. (25) schematically as

$$W(z,\Omega) = - \int_{\infty}^{z} \bar{F}(z',\Omega) dz', \qquad (26)$$

which is independent of z_0. Once $W(z,\Omega)$ is found in this way, $W(z)$ is obtained from $W(z,\Omega)$ using Eq. (7).

To implement a simulation of $\bar{F}(z,\Omega)$ directly requires fixing z and Ω using rigid constraints, and averaging the instantaneous force $F(z,\Omega)$ over a long simulation run, which would ultimately generate the correct equilibrium ensemble average value $\langle F(z,\Omega) \rangle$. $F(z,\Omega)$ fluctuates wildly since there are numerous contributions from the water molecules, ions, and membrane atoms. We present a method which gives reduced noise in the calculation of $\bar{F}(z,\Omega)$. We first relax the constraints somewhat; we employ instead fairly stiff constraints (called restraints), using a few harmonic springs with large force constants. On average the net force $\bar{F}(z,\Omega)$ on the peptide due to the "solvent" (i.e., water, ions, membrane) is balanced by that due to the restraints $\bar{F}^{res}(z,\Omega)$, i.e., $\bar{F}(z,\Omega)+\bar{F}^{res}(z,\Omega)=0$, so that we can obtain $\bar{F}(z,\Omega)$ indirectly using

$$\bar{F}(z,\Omega) = -\bar{F}^{res}(z,\Omega). \qquad (27)$$

The springs record smaller fluctuations than those of the direct forces due to the inertia of the particles attached to the springs. In practice we use restraint springs on three peptide atoms to restrain the peptide center of mass and orientation. Since the peptide is "restrained," rather than "constrained," z and Ω are now mean values. In practice, because we use stiff restraints, the mean values differ very little from the initial (constrained) values.

In our studies the LFCinB peptide and the membrane are restrained in space and the average total force exerted on both the LFCinB and membrane harmonic restraints are monitored and averaged. We confirmed that faster convergence and smaller errors are found by computing restraint forces, compared to computing directly the average total force exerted by the solvent on LFCinB. We find the thermal fluctuations in $F^{res}(z,\Omega)$ to be approximately three to four times smaller than those in $F(z,\Omega)$. Furthermore, by including restraint forces on the membrane as well, the convergence rate is further improved. Other force methods have been employed in [16] and [17]. In [16] and [17] the relative distance between two species is fixed through a holonomic constraint, which is suitable for small molecules where the rotational degrees of freedom are less hindered.

There is one disadvantage to calculating $\bar{F}(z,\Omega)$ indirectly via $\bar{F}^{res}(z,\Omega)$; the decomposition of $\bar{F}(z,\Omega)$ into components (e.g., electrostatic and van der Waals) cannot be obtained from $\bar{F}^{res}(z,\Omega)$. Thus for our quantitative results for $\bar{F}(z,\Omega)$ and $W(z,\Omega)$ we use $\bar{F}^{res}(z,\Omega)$ because of the smaller error bars, but for our qualitative discussion of the contributions to $\bar{F}(z,\Omega)$ and $W(z,\Omega)$ for some typical cases, we use the less accurate direct "solvent" force method.

III. MD SIMULATION

A. General computational details

Our computer simulations are carried out on the multi-institutional high performance computing network, SHARCNET [19], using the program CHARMM [20] with the PARAM27 force field [21]. The van der Waals interactions are smoothly switched off over a distance of 4 Å, between 8 and 12 Å. The electrostatic interactions are simulated using Ewald summation with no truncation [22]. During *NVT* dynamics bond lengths involving hydrogen atoms are constrained with the SHAKE algorithm [23] thus allowing the use of a time step of 2 fs. The water molecules are simulated using the TIP3P water potential [24], where TIP3P is an abbreviation for "transferable intermolecular potential–three point charges."

B. Test of PMF algorithm

Our algorithm is first checked by comparing to the literature results for the PMF $W(r)$ of a Na^{+}-Cl^{-} pair dissolved in water, where r is the pair separation. MD simulations of a Na^{+}-Cl^{-} pair of ions with 216 TIP3P water molecules were carried out with CHARMM using a simulation box with dimensions of $18.856 \times 18.856 \times 18.856$ Å. The temperature of the system is set to 310 K and the two ions are each restrained with springs with force constant 100 $(kcal/mol)/Å^{2}$. Thirty 0.5 ns MD simulations are carried out to determine the PMF (a free energy profile) for the Na^{+}-Cl^{-} pair as a function of the separation, ranging from 2.4 Å to 8.0 Å. The resulting PMF is displayed in Fig. 2. We find that the PMF has two minima. One minimum is observed at $r \sim 3$ Å corresponding to an ionic contact solute
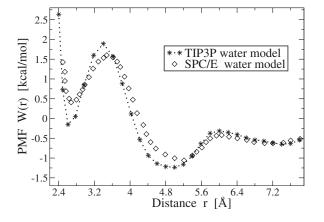
FIG. 2. PMF $W(r)$ for Na$^+$-Cl$^-$ in water box with edge length 18.856 Å containing 216 water molecules at T=300 K. Our result is based on the TIP3P water model, and the result of Ref. [17] is based on the SPC/E water model.

pair (CSP), and a second minimum at $r \sim 5$ Å corresponds to a solvent separated solute pair (SSSP). Moreover, the second minimum is deeper by ~ 1 kcal/mol, and is hence more stable. Our PMF is in good agreement with a simulated result based on constraining the solute pair separation using the SHAKE algorithm [17], with an estimated error of 5–10 %. The small discrepancies between our result and that of Ref. [17] may be due to use of a different water model (SPC/E [25] vs TIP3P [24] used by us), or to spurious mass factors included in the solute-solvent force expression used in Ref. [17]. Here SPC/E is an abbreviation for "simple point charge extended." (The method used in Ref. [17] is that of Ref. [16]; as expected, the latter reference does *not* have mass factors in the expression for the force.) According to results obtained by the traditional weighted histogram method (WHAM) [26] the first minimum is deeper (see, for example, Table II in [17]) which is inconsistent with the experimentally observed fact that NaCl salt easily dissolves in water.

C. Microscopic models for LFCinB peptide and POPC membrane

We simulate a solvated lipid bilayer system of 128 POPC lipids (i.e., 64 lipids in each leaflet) with one LFCinB peptide with its center of mass positioned at a fixed distance from the membrane surface and fixed orientation. LFCinB is a 25-residue antimicrobial peptide with a net charge of $+8e$, where e is the proton charge, with ionized carboxylic and amino groups reflecting the typical protonation state at neutral pH. The NMR-determined crystallographic structure of LFCinB from [6] is available in the Protein Data Bank (PDB code: 1lfc) [27] and is used as the initial structure (Fig. 3). Our POPC simulations using CHARMM are based on the final configuration after a 30 ns MD simulation using GROMACS [28]. The simulation box has dimensions of 64.841×63.993 ×112.0 Å with periodic boundary conditions. The mean distance d between phosphorous atoms in the two membrane leaflets (see Fig. 1) is 36.8 Å [29]. The total number of TIP3P water molecules is 9645 and the water number density is 0.0334 molecules/Å^3, corresponding to mass density of
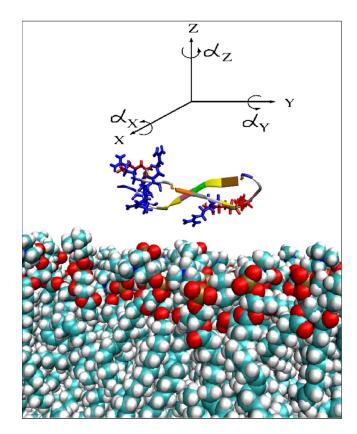

FIG. 3. (Color online) Snapshot of molecular structure showing the initial orientation, of the six principal ones studied, of LFCinB near the upper leaflet of the POPC membrane. The oxygen atoms of the phosphocholine headgroups are shown as red spheres and the phosphorous head group atoms (slightly visible) are in gold. The carbon and hydrogen tail group atoms are shown as white and blue spheres, respectively. The inserted (right-handed) space-fixed axes illustrate the Tait-Bryan angles α_x, α_y, α_z which are used to specify the peptide orientation Ω. In the notation $\Omega=(\alpha_x,\alpha_y,\alpha_z)$ used in Figs. 4 and 5, Ω denotes the orientation with respect to $\alpha_x=0, \alpha_y=0, \alpha_z=0$ shown above. (The conventional right-handed positive rotation angles are indicated by the curved arrows.) The orientation shown [$\Omega=(0,0,0)$] has most of the peptide basic residues [i.e., 5 Arg (in blue) and 3 Lys (in red)] facing the membrane.

0.9983 gm/cm^3. The temperature of the system is set to 310 K, above the gel-liquid crystal phase transition of POPC.

Subsequently, 18 sodium ions and 18 chlorine ions are added with each ion taking the place of a randomly chosen water molecule to create approximately a 0.1 M physiological salt solution. In addition eight chlorine counterions are added to neutralize the simulated system. The total number of chlorine ions is then 26, and the number of sodium ions 18. A set of 72 simulations for different LFCinB configurations with respect to the membrane (12 distances between the LFCinB center of mass and the membrane surface and 6 principal peptide orientations) are carried out. The total number of atoms in the system is 46 588.

IV. CONSTRUCTION OF PMF FOR PEPTIDE-MEMBRANE INTERACTION

In this section we present the methodology for the calculations of the position and orientation PMF $W(z,\Omega)$, the po-

sition PMF $W(z)$, and the binding free energy for LFCinB peptide adsorption on a POPC membrane in a 0.1 M salt solution. The distance z is the distance from the peptide center of mass to the membrane surface, defined as the surface containing the mean positions of the phosphate atoms of the upper leaflet. Since we restrict ourselves to six principal peptide orientations, it is convenient to specify the orientation by the three Tait-Bryan angles, $\Omega = (\alpha_x, \alpha_y, \alpha_z)$, see Fig. 3. To carry out rotations of the peptide we use space-fixed axes x, y, z with origin at the peptide center of mass (displaced for clarity in Fig. 3), x, y axes in the plane parallel to the membrane, and the z axis perpendicular to the membrane plane. The initial peptide orientation shown in Fig. 3 has the peptide backbone along y, and the disulfide bond lies in the x, y plane.

The orientational PMF $W(z, \Omega)$ has been evaluated for the following six principal orientations:

$$\Omega = (0,0,0),(0,90\,°,0),(0,180\,°,0),$$
$$(0,270\,°,0),(90\,°,0,0),(270\,°,0,0).$$

As we see, the first four correspond to "roll" rotations of the peptide around the y axis parallel to the membrane surface through angles $\alpha_y = 0°, 90°, 180°, 270°$, respectively, and the last two are "pitch" rotations about the x axis of $\alpha_x = 90°$ and 270°. The 90° pitch rotation corresponds a configuration in which the peptide backbone is perpendicular to the membrane and the C and N termini are toward the surface. Because of the symmetry of the system we need not rotate the peptide around the z axis ("yaw" rotations). The peptide center of mass–membrane surface separation z ranges from 14 to 36 Å with increments of 2 Å. The simulation procedure is broken down into several stages:

(i) For a given orientation Ω the LFCinB peptide in the bulk is first separated from the membrane to a distance of 36 Å and is constrained in space. The POPC membrane center of mass is harmonically restrained with a spring with force constant 100 (kcal/mol)/Å². The system is equilibrated over 100 ps.

(ii) To create 72 simulation boxes for 12 different positions and 6 different orientations of the LFCinB-POPC system, harmonic restraint forces are applied to the all peptide backbone atoms and the anchor points of these restraints are then moved along the z direction for 100 ps for each step, to decrease the center of mass mean distance by steps of 2 Å, keeping the orientation Ω and the membrane fixed at each step.

(iii) After creating the 72 initial systems each of them is equilibrated for 500 ps. During this equilibration and data collection the LFCinB peptide is orientationally restrained using harmonic springs coupled to the three carbon C_α backbone atoms of CYS3, CYS20, and PRO16. All spring constants are 100 (kcal/mol)/Å². To a good approximation the peptide center of mass is held on average at the same position as generated by the steps in (ii).

(iv) The instantaneous restraint forces are computed during 2.5 ns trajectories for each of the 72 system configurations with sampling interval of 0.2 ps, and averaged to obtain the mean force $\bar{F}(z, \Omega) = -\bar{F}^{res}(z, \Omega)$ for each center of mass

mean position z, which is also monitored. The PMF $W(z, \Omega)$ is calculated from $\bar{F}(z, \Omega)$ using Eq. (26), where integration over the z coordinate is performed using the trapezoidal rule. We note again that the mean values of z and Ω differ very little from the original (constrained) assigned values.

The PMF at the initial position $z = z_0$ can be estimated from the Lifshitz theory of long range van der Waals forces applied for molecule-surface interactions [30,31] using the value of the Hamaker constant for POPC-LFCinB interacting through water obtained from the models of [30,31]. The estimated value of $W(z_0)$ is negative and smaller in magnitude than 10^{-2} kcal/mol for $z_0 = 36$ Å, so it is a reasonable approximation to assume that $W(z_0) = 0$ for $z_0 \gtrsim 36$ Å.

The MD simulations of the forces acting on LFCinB and the calculations of the six independent profiles $W(z, \Omega)$ took about 250 000 cpu hours. $W(z)$ is obtained from $W(z, \Omega)$ using Eq. (7); for each value of z, we perform an unweighted average of the six simulated values of $\exp[-\beta W(z, \Omega)]$ to obtain $\exp[-\beta W(z)]$.

Great effort is made to reduce the statistical errors. A difficulty is that, on short time scales, the results are highly correlated, and thus unsuitable for statistical analysis. We find that the correlation time for estimating the error due to solvent force fluctuations is about 0.1 ns, and membrane fluctuations and systematic error due to the harmonic restraints require data for not less than 0.5 ns to compute reliable average forces. The total sampling time must therefore be long enough to ensure a collection of uncorrelated configurations. Using the block-averaging method [32] we find the statistical errors in $\bar{F}(z, \Omega)$ to be within 0.35 (kcal/mol)/Å in all cases. In addition to the statistical error there may be systematic errors due to errors in the CHARMM force field, and to the limited number of peptide orientations sampled.

V. RESULTS AND ANALYSIS

Figures 4 and 5 show the results of the simulation of the PMF $W(z, \Omega)$ for LFCinB-POPC interactions. For clarity, in Fig. 4 we display the PMF $W(z, \Omega)$ for the four orientations Ω in which the peptide backbone is parallel to the membrane, and in Fig. 5 $W(z, \Omega)$ is given for the two peptide orientations in which the peptide backbone is perpendicular to the membrane.

We find, as displayed in Fig. 4, that the PMF for $\Omega = (0, 90°, 0)$ has the minimum energy profile, in which the peptide backbone is parallel to the membrane and the side facing the membrane contains most of the aromatic residues. The first and the second PMF minima are almost the same and not very deep, ≈ -2.0 kcal/mol for this orientation, and thus the zwitterionic POPC membrane forms a relatively weak (compared to charged membranes) binding complex with LFCinB. The least attractive (here purely repulsive) profile with $\Omega = (90°, 0, 0)$, shown in Fig. 5, has the peptide backbone perpendicular to the membrane with C and N termini toward the surface. The curves for the other orientations simulated [i.e., $\Omega = (0,0,0),(0,180°,0),(0,270°,0),(270°,0,0)$] lie between those shown, as illustrated in Figs. 4 and 5.
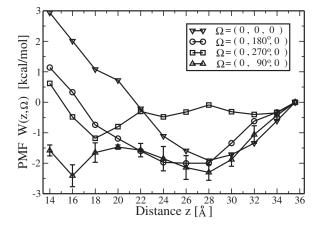
FIG. 4. PMF $W(z,\Omega)$ for LFCinB-POPC system for four peptide orientations Ω in which the peptide backbone is parallel to the membrane. z is the distance between the LFCinB center of mass and the membrane surface. The notation $\Omega=(\alpha_x,\alpha_y,\alpha_z)$ is explained in the caption to Fig. 3. LFCinB with orientation $\Omega=(0,90°,0)$ has the minimum energy profile with the side facing the membrane containing most of the aromatic residues. Each data point represents the mean of five 0.5 ns simulations of $W(z,\Omega)$, and the error bars represent the dispersion among the five. The curves for the perpendicular orientations simulated are shown separately in Fig. 5.

To understand the detailed moleculer mechanism of interaction between peptide and membrane we decompose the free energy in terms of van der Waals and electrostatic contributions; decomposition in terms of enthalpic and entropic components is also given. Because the system is nonuniform in the z direction it is useful to consider separately three regions of the PMF. The dividing lines between the regions are somewhat arbitrary; for $z<20$ Å the forces are repul-
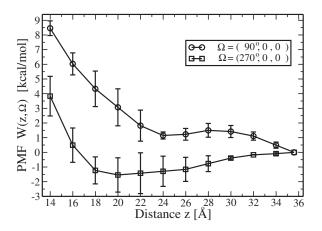

FIG. 5. PMF $W(z,\Omega)$ for LFCinB-POPC system for two peptide orientations Ω in which the peptide backbone is perpendicular to the membrane. z is the distance between the LFCinB center of mass and the membrane surface. The notation $\Omega=(\alpha_x,\alpha_y,\alpha_z)$ is explained in the caption to Fig. 3. The least attractive (here purely repulsive) profile with $\Omega=(90°,0,0)$ has the C and N termini toward the surface. Each data point represents the mean of five 0.5 ns simulations of $W(z,\Omega)$, and the error bars represent the dispersion among the five. The curves for the parallel orientations simulated are shown separately in Fig. 4.
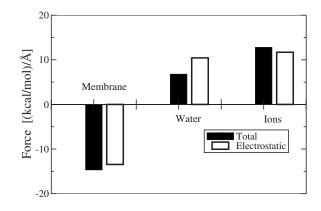

FIG. 6. Decomposition of the average net force acting on the peptide with orientation $\Omega=(0,90°,0)$ due to the "solvent," averaged over a 2.5 ns simulation for the distance $z=18$ Å between the LFCinB center of mass and the membrane surface. Negative and positive forces correspond to peptide-membrane attraction and repulsion, respectively. The total mean forces on the peptide, as well as the electrostatic contributions, due to the water, ions, and membrane, are shown.

sive, and for $z>28$ Å, the forces are weak and attractive (van der Waals dispersion forces).

(i) Contact region ($14<z<20$ Å). This is the region where the direct peptide-membrane electrostatic interactions and van der Waals repulsive forces play the dominant role.

(ii) Intermediate region ($20<z<28$ Å). There are indirect interactions of LFCinB with the membrane due to unsymmetrical distributions of water and ions around the LFCinB.

(iii) Far region ($z>28$ Å). This is the region in which we have predominantly weak attractive interactions presumably due to the van der Waals dispersion forces.

In the contact region the MD simulations play a crucial role in understanding the mechanisms of interaction on the molecular level where continuum theory fails. To decompose the force into components, we must use the less accurate "direct solvent" method, as discussed in Sec. II C. Decomposition of the forces acting on the LFCinB in the contact region for the two peptide orientations $\Omega=(0,90°,0)$ and $(0,180°,0)$ into system components (membrane, water, ions) and type of interaction (electrostatic, van der Waals) provides insight into the nature of the dominant contributions to the PMF. The calculation of the forces from different components of the system for the $\Omega=(0,90°,0)$ peptide orientation (the most attractive one) shows (Fig. 6) that the only source of the attractive force acting on the LFCinB in this region is the direct membrane-peptide interaction. We see from Fig. 6 that for the distance $z=18$ Å this attractive force is at least four times larger than the average total force acting on the LFCinB and is due almost entirely to electrostatics. The van der Waals component of the direct membrane-peptide interaction is negligible in this region; the van der Waals attraction of most of the peptide residues is compensated by the overlap repulsion of a few residues which are in contact with membrane atoms. The sources of the cancellation of the direct membrane-peptide electrostatic interaction in the contact region are discussed in the next two paragraphs.

Ion-peptide interactions in the contact region give rise to large repulsive forces acting on LFCinB. This repulsion is a result of the change in the counterion distribution around LFCinB during its approach to the membrane. The average number of counterions in the region between LFCinB and the membrane decreases with decreasing z leading to less attraction from the membrane side of the peptide, and thus a net repulsion. Therefore the ions induce net repulsive forces in this region.

The water-peptide interaction provides a net repulsive mean force in the contact region, also contributing to the near cancellation of the direct attractive membrane-peptide interaction. This repulsion, as with the ion-peptide repulsion, is a consequence of the change in the water distribution around LFCinB during its approach to the membrane. The net force resulting from the water is smaller than the forces due to the membrane and the ions. This force is a result of a competition between a repulsive electrostatic contribution and a mostly attractive van der Waals contribution.

The calculation of the forces from different components of the system for the $\Omega = (0, 180°, 0)$ peptide orientation exhibit the same qualitative behavior (we do not present the details), although the amplitudes of the electrostatic and van der Waals contributions are substantially greater than in the case of the $(0,90°,0)$ orientation.

From a macroscopic point of view, the simulations are consistent with the often-stated view [31] that when a charged peptide moves toward a neutral membrane, counterions and water molecules are forced into a smaller space, decreasing their entropy and giving rise to a repulsive interaction force at short range. The enthalpy cost to desolvate the ions and water from the peptide and membrane as the peptide is pushed toward the membrane also contributes to the short range repulsive force. The entropy and enthalpy contribution to the interaction are discussed further below.

In the mid and far regions the values of the contributions to the total force are smaller than their statistical errors found in the force analysis of the simulations. Therefore no conclusions about the dominant contributions to the net force can be drawn from the simulations. However, we know from the general Derjaguin-Landau-Verwey-Overbeek (DLVO) and Lifshitz theories (see, e.g., [31,33]) of long-range interactions that the van der Waals dispersion force is the major source of the attraction between a charged molecule (here a peptide) and a neutral surface at large distances.

Figure 7 shows the orientationally averaged PMF $W(z)$. There are two minima which are of nearly equal depth and separated by approximately 10 Å. Because $W(z)$ is related to the local density $\rho(z)$ by Eq. (8), this suggests that a "layering" effect may occur for LFCinB near POPC membranes.

The decomposition of the free energy profile $W(z)$ into enthalpic $[\Delta H(z)]$ and entropic $[-T\Delta S(z)]$ components is carried out using Eqs. (20) and (21) and is shown in Fig. 7. Note that $-T\Delta S(z)$ is smaller in magnitude than $\Delta H(z)$ and has opposite sign, so that the binding is enthalpy driven. The net negative value of $\Delta S(z)$ is the resultant [8] of negative contributions (i.e., loss of translational, overall rotational, and internal rotational freedom of the peptide) and positive contributions (i.e., partial dehydration of peptide and membrane,
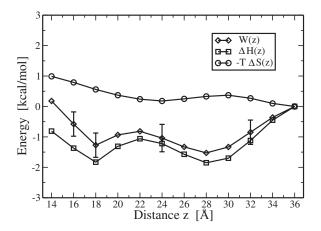

FIG. 7. Decomposition of the free energy profile (PMF) $W(z)$, for LFCinB-POPC binding, into enthalpic $[\Delta H(z)]$ and entropic $[-T\Delta S(z)]$ components. z is the distance between the LFCinB center of mass and the membrane surface.

and peptide and membrane vibrational frequency shifts to lower values).

Using Eqs. (14) and (15) and choosing the range of the binding region to be $\Delta l = 22$ Å (corresponding to $l' = 14$ Å and $l = 36$ Å) we find a binding free energy of $\Delta G^0 = -1.05 \pm 0.39$ kcal/mol with the enthalpic and entropic contributions $\Delta H^0 = -1.48 \pm 0.31$ kcal/mol and $-T\Delta S^0 = +0.43 \pm 0.24$ kcal/mol, respectively, calculated from Eqs. (22) and (23). The binding is relatively weak, compared to that for charged membranes. Expressed in the terms of the forces involved, from the slopes in Fig. 4 we find the maximum average attractive force to be about 0.3 (kcal/mol)/Å, or 20 pN.

VI. CONCLUSIONS

We use a new variant of the combination constrained MD and thermodynamic integration to simulate the PMF for LFCinB-POPC binding. We calculate the binding constant, which depends only on molecular characteristics and the actual state conditions, namely the PMF $W(z)$, independent of the choice of standard state and independent of any additional adjustable parameters, such as an arbitrary cutoff of the binding region. Using this approach we predict the binding free energy to be $\Delta G^0 = -1.05 \pm 0.39$ kcal/mol, and a corresponding maximum binding force of about 20 pN, for LFCinB-POPC in a 100 mM salt solution at 310 K. The most favorable orientation of LFCinB has most of the aromatic residues facing the membrane. Experiments could be carried out to check our predictions for the observables ΔG^0 and ΔH^0 using, for example, isothermal titration calorimetry.

From the point of view of selecting a peptide as a potential antimicrobial one, the relatively weak binding found here for LFCinB-POPC is encouraging since POPC resembles somewhat mammalian membranes, and it is required to find peptides which cause minimal damage to mammals. Conversely, it is required to find peptides which interact strongly with bacterial-like (comparatively strongly charged) membranes (e.g., POPG), which LFCinB appears to do (see below).

This study will be a useful starting point for simulating peptides interacting with charged anionic phosphatidylglycerol membranes and interactions involved in peptide penetration of membranes. Preliminary results of simulations by us involving the charged POPG membrane indicate a much stronger binding for LFCinB-POPG as expected from electrostatic arguments [34]. Further simulations of peptide-membrane systems, particularly the penetration region, will give some insight into the mechanisms leading to peptide-induced membrane disruption and membrane-peptide selectivity, features necessary to understand in order to rationally design novel antimicrobial peptides.

APPENDIX: THE PMF THEOREM

The PMF theorem relates, for a system in equilibrium, the mean force on a coordinate or set of coordinates to the derivative of the PMF W with respect to one of its arguments. In the simplest cases involving only Cartesian coordinates [37], the relation is $\langle \mathbf{F}_1 \rangle_1 \equiv \langle -\partial U / \partial \mathbf{r}_1 \rangle_1 = -\partial W(\mathbf{r}_1) / \partial \mathbf{r}_1$, where $\mathbf{r}_1$ is one of the coordinates (say the first) of the system's set of n Cartesian coordinates $(\mathbf{r}_1, \mathbf{r}_2, \ldots, \mathbf{r}_n)$, and $\langle \cdots \rangle_1$ denotes an ensemble average with $\mathbf{r}_1$ held fixed, i.e., $\langle \cdots \rangle_1 = \int d\mathbf{r}_2 \cdots d\mathbf{r}_n P(\mathbf{r}_2, \ldots, \mathbf{r}_n | \mathbf{r}_1)(\cdots)$, where $P(\mathbf{r}_2, \ldots, \mathbf{r}_n | \mathbf{r}_1) \equiv P(\mathbf{r}_1, \mathbf{r}_2, \ldots, \mathbf{r}_n) / P(\mathbf{r}_1)$ is the conditional probability density to find $(\mathbf{r}_2, \ldots, \mathbf{r}_n)$ given $\mathbf{r}_1$, $P(\mathbf{r}_1, \mathbf{r}_2, \ldots, \mathbf{r}_n) = \exp[-\beta U(\mathbf{r}_1, \mathbf{r}_2, \ldots, \mathbf{r}_n)] / Z$ is the full normalized configurational distribution function, $Z = \int d\mathbf{r}_1 \cdots d\mathbf{r}_n \exp[-\beta U(\mathbf{r}_1, \mathbf{r}_2, \ldots, \mathbf{r}_n)]$ is the configurational partition function, $U(\mathbf{r}_1, \ldots, \mathbf{r}_n)$ is the system potential energy, and $P(\mathbf{r}_1) = \int d\mathbf{r}_2 \cdots d\mathbf{r}_n P(\mathbf{r}_1, \mathbf{r}_2, \ldots, \mathbf{r}_n)$ is the singlet distribution function. The PMF $W(\mathbf{r}_1)$ is defined by $P(\mathbf{r}_1) \equiv C \exp[-\beta W(\mathbf{r}_1)]$, where $C^{-1} = \int d\mathbf{r}_1 \exp[-\beta W(\mathbf{r}_1)] \approx V$ is the normalization constant, with V the system volume. We are restricting ourselves to classical statistical mechanics and have therefore used the classical form for $P(\mathbf{r}_1, \mathbf{r}_2, \ldots, \mathbf{r}_n)$.

If a change of variables is made to non-Cartesian or generalized coordinates, in general the form of the PMF theorem is more complicated [18] since it involves the Jacobian of the transformation. In Sec. II we made the change of variables from $(\mathbf{r}_1, \mathbf{r}_2, \ldots, \mathbf{r}_n)$ to $(\mathbf{r}, \Omega, q)$, where $\mathbf{r}, \Omega$ are the peptide center of mass position and overall orientation (i.e., six variables including three non-Cartesian ones), and q denotes all remaining system coordinates, i.e., peptide internal (vibrational) coordinates (possibly non-Cartesian), water atom, ion, and membrane atom coordinates. Here we show that this particular change of variables leaves intact the simple form of the PMF theorem despite the fact that it involves some non-Cartesian variables.

To simplify the proof we choose the peptide $\mathbf{r}, \Omega$ coordinates as follows: $\mathbf{r}$ is taken to be the position $\mathbf{r}_1$ of atom 1 (arbitrarily chosen) of the peptide (a later Cartesian shift to the center of mass is harmless), and Ω denotes the Euler angles giving the orientation of the triangle formed by atoms 1, 2, and 3 of the peptide, where again atoms 2 and 3 are chosen arbitrarily (but noncolinear with atom 1). Internal coordinates of the peptide are with respect to the body-fixed axes x', y', z', with origin at atom 1 and where x', y' are in the plane of the triangle, and z' is perpendicular to the triangle. All other (i.e., nonpeptide) system coordinates are left unchanged.

The relation we seek to establish is

$$\left\langle \frac{\partial U}{\partial z} \right\rangle_{z,\Omega} = \frac{\partial W(z,\Omega)}{\partial z}, \tag{A1}$$

where z is the z coordinate of $\mathbf{r} = (x, y, z)$, $W(z, \Omega)$ is the PMF, $U(z, \Omega, q)$ is the system potential energy expressed as a function of the new variables, and where we have absorbed the x, y coordinates of $\mathbf{r}$ into q. The notation $\langle \cdots \rangle_{z,\Omega}$ indicates an average over the conditional distribution function $P(q|z,\Omega) \equiv P(z,\Omega,q) / P(z,\Omega)$ to find q given z, Ω, i.e.,

$$\left\langle \frac{\partial U}{\partial z} \right\rangle_{z,\Omega} = \int dq \frac{P(z,\Omega,q)}{P(z,\Omega)} \frac{\partial U}{\partial z}, \tag{A2}$$

where $P(z,\Omega) \equiv \int dq P(z,\Omega,q)$ is a reduced distribution function. The system full distribution function $P(z,\Omega,q)$ is related to the original one, $P(\mathbf{r}_1, \mathbf{r}_2, \ldots, \mathbf{r}_n) = \exp[-\beta U(\mathbf{r}_1, \mathbf{r}_2, \ldots, \mathbf{r}_n)] / Z$, by

$$P(z,\Omega,q) = |J| \frac{e^{-\beta U(z,\Omega,q)}}{Z}, \tag{A3}$$

where

$$Z = \int d\mathbf{r}_1 \cdots d\mathbf{r}_n \exp[-\beta U(\mathbf{r}_1, \ldots, \mathbf{r}_n)]$$

$$= \int dz\, d\Omega\, dq\, |J| \exp[-\beta U(z,\Omega,q)],$$

and $|J|$ is the magnitude of the Jacobian determinant J of the transformation $(\mathbf{r}_1, \mathbf{r}_2, \ldots, \mathbf{r}_n) \rightarrow (z, \Omega, q)$. The important fact to note about J is that it is independent of $\mathbf{r}$ (and hence z) since the transformation $\mathbf{r} = \mathbf{r}_1$ is Cartesian so that $\partial \mathbf{r} / \partial \mathbf{r}_1$ is independent of $\mathbf{r}$.

From Eqs. (A2) and (A3) and the fact that J is independent of z we get

$$\left\langle \frac{\partial U}{\partial z} \right\rangle_{z,\Omega} = \frac{1}{P(z,\Omega)} \int dq \frac{|J| e^{-\beta U(z,\Omega,q)}}{Z} \frac{\partial U}{\partial z}$$

$$= -\frac{1}{\beta P(z,\Omega)} \frac{\partial}{\partial z} \int dq \frac{|J| e^{-\beta U(z,\Omega,q)}}{Z}$$

$$= -\frac{1}{\beta P(z,\Omega)} \frac{\partial}{\partial z} P(z,\Omega) = -\frac{1}{\beta} \frac{\partial}{\partial z} \ln P(z,\Omega). \tag{A4}$$

The PMF $W(z,\Omega)$ is defined by

$$P(z,\Omega) \equiv Ce^{-\beta W(z,\Omega)}, \tag{A5}$$

where $C^{-1} = \int dz d\Omega \exp[-\beta W(z,\Omega)] \approx 8\pi^2 L$ is the normalization constant for the distribution function $P(z,\Omega)$. From Eq. (A5) we get

$$-\frac{1}{\beta}\frac{\partial}{\partial z}\ln P(z,\Omega) = \frac{\partial W(z,\Omega)}{\partial z}. \tag{A6}$$

Substituting Eq. (A6) into Eq. (A4) gives the desired relation (A1). Note that Eq. (A1) has the simple form, independent of J. By measuring the mean force $\bar{F}(z,\Omega) \equiv \langle -\partial U / \partial z \rangle_{z,\Omega} = -\partial W(z,\Omega)/\partial z$ in the simulation at a series of values $z = z'$, we obtain $W(z,\Omega)$ by integration using Eq. (26) of the text.

[1] http://www.bbcm.univ.trieste.it/ tossi/amsdb.html
[2] M. Zasloff, Nature (London) **415**, 389 (2002).
[3] *Mammalian Host Defense Peptides*, edited by D. A. Devine and R. E. W. Hancock (Cambridge University Press, Cambridge, England, 2004).
[4] K. Matsuzaki, Biochim. Biophys. Acta **1462**, 1 (1999).
[5] H. J. Vogel, D. J. Shibili, W. Jing, E. M. Lohmeier-Vogel, R. F. Epand, and R. M. Epand, Biochem. Cell Biol. **80**, 49 (2002).
[6] P. M. Hwang, N. Zhou, X. Shan, C. H. Arrowsmith, and H. J. Vogel, Biochemistry **37**, 4288 (1998).
[7] P. H. Nibbering, E. Ravensbergen, M. M. Welling, L. A. van Berkel, P. H. C. van Berkel, E. K. J. Paulwels, and J. H. Nuijens, Infect. Immun. **69**, 1469 (2001).
[8] M. K. Gilson, J. A. Given, B. L. Bush, and J. A. McCammon, Biophys. J. **72**, 1047 (1997).
[9] N. Ben-Tal, B. Honig, C. K. Bagdassarian, and A. Ben-Shaul, Biophys. J. **79**, 1180 (2000).
[10] B. Widom, *Statistical Mechanics* (Cambridge University Press, Cambridge, England, 2002), p. 170.
[11] H. L. Friedman and C. V. Krishman, in *Water*, edited by F. Franks (Plenum, New York, 1973), Vol. 3, p. 1.
[12] W. A. Steele, Surf. Sci. **36**, 317 (1973).
[13] *Free Energy Calculations*, edited by C. Chipot and A. Pohorille (Springer, Berlin, 2007).
[14] D. J. Tobias and C. L. Brooks III, Chem. Phys. Lett. **142**, 472 (1987).
[15] B. Roux and M. Karplus, Biophys. J. **59**, 961 (1991).
[16] G. Ciccotti, M. Ferrario, J. T. Hynes, and R. Kapral, Chem. Phys. **129**, 241 (1989).
[17] H. Shinto, S. Morisada, M. Miyahara, and K. Higashitani, J. Chem. Eng. Jpn. **36**, 57 (2003).
[18] E. Darve, in *Free Energy Calculations*, edited by C. Chipot and A. Pohorille (Springer, Berlin, 2007), p. 119.

[19] http://www.sharcnet.ca
[20] B. R. Brooks, R. E. Brucolleri, B. D. Olafson, D. J. States, S. Swaminathan, and M. Karplus, J. Comput. Chem. **4**, 187 (1983).
[21] A. D. MacKerell, D. Bashford, M. Bellot, R. L. Dunbrack, and J. Evanseek, J. Phys. Chem. B **102**, 3586 (1998).
[22] J. Kolafa and J. W. Perram, Mol. Simul. **9**, 351 (1992).
[23] J. P. Ryckaert, G. Ciccotti, and H. J. C. Berendsen, J. Comput. Phys. **23**, 327 (1977).
[24] W. L. Jorgensen, J. Chandrasekhar, J. D. Madura, R. W. Impey, and M. L. Klein, J. Chem. Phys. **79**, 926 (1983).
[25] H. J. C. Berendsen, J. R. Grigera, and T. P. Straatsma, J. Phys. Chem. **91**, 6269 (1987).
[26] S. Crouzy, J. Boudry, J. C. Smith, and B. Roux, J. Comput. Chem. **20**, 1644 (1999).
[27] http://www.rcsb.org
[28] http://www.apmaths.uwo.ca/mkarttu//downloads.shtml
[29] D. E. Elmore, FEBS Lett. **580**, 144 (2006).
[30] J. Israelachvili, *Intermolecular and Surface Forces*, 2nd ed. (Academic, London, 1997), p. 190.
[31] D. F. Evans and H. Wennerstrom, *Colloidal Domain*, 2nd ed. (Wiley VCH, New York, 1999), p. 409.
[32] H. Flyvbjerg and H. G. Petersen, J. Chem. Phys. **91**, 461 (1989).
[33] V. A. Parsegian, *Van der Waals Forces* (Cambridge University Press, New York, 2006).
[34] V. Vivcharuk, B. Tomberli, I. S. Tolokh, and C. G. Gray, Phys. Rev. E (to be published).
[35] http://www.nserc crsng.gc.ca
[36] http://www.afmnet.ca
[37] T. L. Hill, *Statistical Mechanics* (McGraw-Hill, New York, 1956), p. 193.